

Supplementary Information

Evolutionary Stability of Small Molecular Regulatory Networks that Exhibit Near-Perfect Adaptation

Rajat Singhania and John J. Tyson

Outline:

Supplementary Text S1. *A Catalogue of Mechanisms for Robust Perfect Adaptation and Near Perfect Adaptation*

Supplementary Table S1. The *pure* signaling motifs.

Supplementary Table S2. NFLB-1 topologies (1X3X3X) macro-mutate predominantly into high-scoring IFFL-1 + NFLB-1 topologies (1X3X31).

Supplementary Table S3. NFLB-3 topologies (XXX331) macro-mutate predominantly into high-scoring IFFL-1 + NFLB-1 topologies (1X3X31).

Supplementary Table S4. NFLB-2 topologies (3X1X3X) macro-mutate predominantly to high-scoring IFFL-1 + NFLB-1 topologies (1X3X31).

Supplementary Table S5. NFLB-4 topologies (XXX133) macro-mutate predominantly to high-scoring IFFL-1 + NFLB-1 topologies (1X3X31).

Supplementary Table S6. The percentage change in average score $\langle Z \rangle$ going from an *uncoupled* NFLB-1 topology to a coupled NFLB-1 + IFFL-1 topology.

Supplementary Table S7. The percentage change in average score $\langle Z \rangle$ going from an *uncoupled* NFLB-2 topology to a coupled NFLB-2 + IFFL-4 topology.

Supplementary Table S8. The percentage change in average score $\langle Z \rangle$ going from an *uncoupled* NFLB-3 topology to a coupled NFLB-3 + IFFL-1 topology.

Supplementary Table S9. The percentage change in average score $\langle Z \rangle$ going from an *uncoupled* NFLB-4 topology to a coupled NFLB-4 + IFFL-4 topology.

Supplementary Table S10. The percentage changes in average score $\langle Z \rangle$ going from an *uncoupled* IFFL-1 topology to a coupled IFFL-1 + NFLB-1 topology.

Supplementary Table S11. The percentage changes in average score $\langle Z \rangle$ going from an *uncoupled* IFFL-1 topology to a coupled IFFL-1 + NFLB-3 topology.

Supplementary Table S12. The percentage changes in average score $\langle Z \rangle$ going from an *uncoupled* IFFL-1 topology to a coupled IFFL-1 + NFLB-1 + NFLB-3 topology.

Supplementary Table S13. The percentage changes in average score $\langle Z \rangle$ adding an NFLB-3 topology to a coupled IFFL-1 + NFLB-1 topology.

Supplementary Table S14. The percentage changes in average score $\langle Z \rangle$ adding an NFLB-1 topology to a coupled IFFL-1 + NFLB-3 topology.

Supplementary Table S15. The percentage changes in average score $\langle Z \rangle$ going from an *uncoupled* IFFL-4 topology to a coupled IFFL-4 + NFLB-2 topology.

Supplementary Table S16. The percentage changes in average score $\langle Z \rangle$ going from an *uncoupled* IFFL-4 topology to a coupled IFFL-4 + NFLB-4 topology.

Supplementary Table S17. The percentage changes in average score $\langle Z \rangle$ going from an *uncoupled* IFFL-4 topology to a coupled IFFL-4 + NFLB-2 + NFLB-4 topology.

Supplementary Table S18. The percentage changes in average score $\langle Z \rangle$ adding an NFLB-4 topology to a coupled IFFL-4 + NFLB-2 topology.

Supplementary Table S19. The percentage changes in average score $\langle Z \rangle$ adding an NFLB-2 topology to a coupled IFFL-4 + NFLB-4 topology.

Supplementary Table S20. Mean values of the six interaction coefficients from all high-scoring samples of IFFL-1 topologies.

Supplementary Table S21. Mean values of the six interaction coefficients from all high-scoring samples of IFFL-4 topologies.

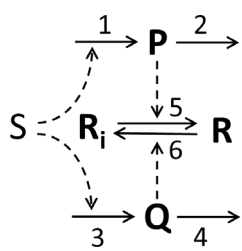
Supplementary Text S1. A Catalogue of Mechanisms for Robust Perfect Adaptation and Near Perfect Adaptation

Each motif is displayed as a reaction network among four species: S, P, Q and R; where S is the ‘signal’ and R is the ‘response’. (In some cases, P and R are combined into one species.) For robust perfect adaptation (RPA), the steady-state concentration of R (i.e., R_{ss}) is independent of the signal strength S, regardless of the kinetic parameter values (provided there exists a steady state solution with all positive concentrations). For near-perfect adaptation (NPA), R_{ss} depends only weakly of S. For many proposed mechanisms, RPA depends on an assumption that particular chemical reactions proceed at a constant rate, independent of the concentration of the reactant. These reactions are indicated by the symbol ($\circ \rightarrow$), and the constant rate of the reaction is denoted by V . For the ‘standard’ reactions in the motifs (symbolized by \rightarrow), the reaction rates are given by the law of mass action, with positive rate constants k_i . The role of the ‘signal’ is often expressed by an arbitrary, monotone increasing function $F(S)$; e.g., $1+S$, or $\frac{S}{1+S}$, or $\frac{S^n}{1+S^n}$.

In cases where Q inhibits a reaction, the rate of the reaction is multiplied by $\frac{1}{1+Q}$, but other monotone decreasing functions would work equally well. In motif #6 below, the T-shaped reaction arrow indicates reversible binding of P + R to yield the complex Q, with forward rate constant k_{3f} and reverse rate constant k_{3r} . The Y-shaped connector in motif #11 denotes irreversible binding.

#	Mechanism	Differential Equations	Steady-State	References
1		$\frac{dP}{dt} = k_1 SR - k_2 P + (1 - \alpha)V_3$ $\frac{dQ}{dt} = k_4 R - V_3$ $\frac{dR}{dt} = \alpha V_3 + k_2 P - k_1 SR - k_4 R$	$P = \frac{V_3}{k_2} \left(1 - \alpha + \frac{k_1 S}{k_4}\right)$ $R = \frac{V_3}{k_4}$ $P + Q + R = \text{const} > 0$	Barkai & Leibler (1997) Khammash (2021)
2		$\frac{dQ}{dt} = k_3 R - V_4$ $\frac{dR}{dt} = \frac{k_1 F(S)}{1+Q} - k_2 R - k_3 R$	$1 + Q = \frac{k_3 k_1 F(S)}{V_4 (k_2 + k_3)} > 1$ $R = \frac{V_4}{k_3}$	Yi et al. (2000) “integral feedback”

3

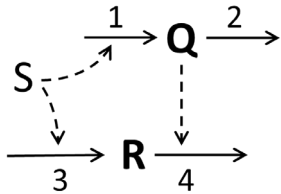


$$\begin{aligned}\frac{dP}{dt} &= k_1 F(S) - k_2 P \\ \frac{dQ}{dt} &= k_3 F(S) - k_4 Q \\ \frac{dR}{dt} &= k_5 P(R_T - R) - k_6 QR\end{aligned}$$

$$\begin{aligned}P &= \frac{k_1 F(S)}{k_2} \\ Q &= \frac{k_3 F(S)}{k_4} \\ R &= \frac{R_T}{1 + \frac{k_2 k_3 k_6}{k_1 k_4 k_5}}\end{aligned}$$

Levchenko &
Iglesias
(2002)

4

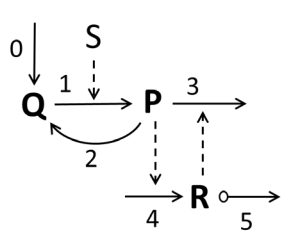


$$\begin{aligned}\frac{dQ}{dt} &= k_1 F(S) - k_2 Q \\ \frac{dR}{dt} &= k_3 F(S) - k_4 QR\end{aligned}$$

$$\begin{aligned}Q &= \frac{k_1 F(S)}{k_2} \\ R &= \frac{k_2 k_3}{k_1 k_4}\end{aligned}$$

Tyson et al.
(2003)
(Fig. 1d)
“Sniffer”

5

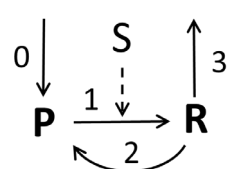


$$\begin{aligned}\frac{dP}{dt} &= k_1 SQ - k_2 P - k_3 RP \\ \frac{dQ}{dt} &= k_0 - k_1 SQ + k_2 P \\ \frac{dR}{dt} &= k_4 P - V_5\end{aligned}$$

$$\begin{aligned}P &= \frac{V_5}{k_4} \\ Q &= \frac{k_0 k_4 + k_2 V_5}{k_4 k_1 S} \\ R &= \frac{k_0 k_4}{k_3 V_5}\end{aligned}$$

Behar et al.
(2007)
(Model IVA)

6

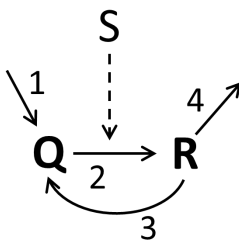


$$\begin{aligned}\frac{dP}{dt} &= k_0 - k_1 F(S)P + k_2 R \\ \frac{dR}{dt} &= k_1 F(S)P - k_2 R - k_3 R\end{aligned}$$

$$\begin{aligned}P &= \frac{k_0(k_2 + k_3)}{k_3 k_1 F(S)} \\ R &= \frac{k_0}{k_3}\end{aligned}$$

Hao et al.
(2007)
Drengstig et
al. (2008)

7

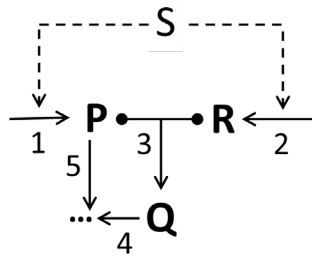


$$\begin{aligned}\frac{dQ}{dt} &= k_1 - k_2 F(S)Q + k_3 R \\ \frac{dR}{dt} &= k_2 F(S)Q - k_3 R - k_4 R\end{aligned}$$

$$\begin{aligned}Q &= \frac{k_1}{k_2 F(S)} \left(1 + \frac{k_3}{k_4}\right) \\ R &= \frac{k_1}{k_4}\end{aligned}$$

Francois &
Siggia (2008)
(Fig. 4)

8



$$\frac{dP}{dt} = k_1 F(S) - k_{3f} PR + k_{3r} Q - k_5 P$$

$$\frac{dQ}{dt} = k_{3f} PR - k_{3r} Q - k_4 Q$$

$$\frac{dR}{dt} = k_2 F(S) - k_{3f} PR + k_{3r} Q$$

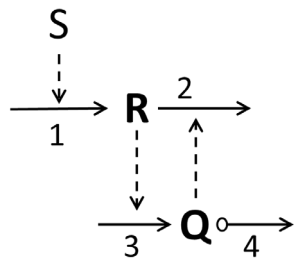
$$P = \frac{(k_1 - k_2)F(S)}{k_5}$$

$$Q = \frac{k_2 F(S)}{k_4}$$

$$R = \frac{k_2 k_5 (k_{3r} + k_4)}{k_4 (k_1 - k_2) k_{3f}}$$

Francois &
Siggia (2008)
(Fig. 7)

9



$$\frac{dQ}{dt} = k_3 R - V_4$$

$$\frac{dR}{dt} = k_1 F(S) - k_2 QR$$

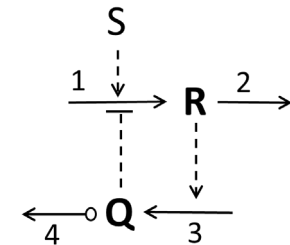
$$Q = \frac{k_1 F(S)}{k_2} \cdot \frac{k_3}{V_4}$$

$$R = \frac{V_4}{k_3}$$

Behar et al.
(2007)
(Model I)

Ni et al.
(2009)
(Fig. 6a)

10



$$\frac{dQ}{dt} = k_3 R - V_4$$

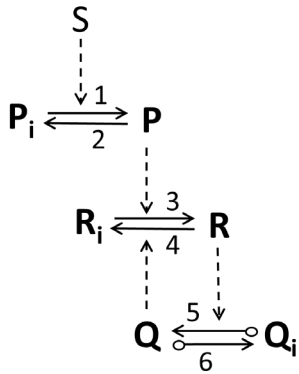
$$\frac{dR}{dt} = \frac{k_1 F(S)}{1+Q} - k_2 R$$

$$1 + Q = \frac{k_1 F(S)}{k_2} \cdot \frac{k_3}{V_4} > 1$$

$$R = \frac{V_4}{k_3}$$

Ni et al.
(2009)
(Fig. 6b)

11



$$\frac{dP}{dt} = k_1 S(1 - P) - k_2 P$$

$$\frac{dQ}{dt} = k_5 R - k_6$$

$$\frac{dR}{dt} = k_3 P(1 - R) - k_4 QR$$

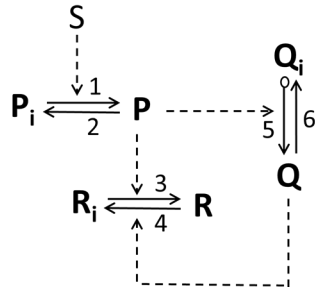
$$P = \frac{k_1 S}{k_1 S + k_2}$$

$$Q = \frac{k_3 (k_5 - k_6)}{k_4 k_6} \left(\frac{k_1 S}{k_1 S + k_2} \right)$$

$$R = \frac{k_6}{k_5} < 1$$

Ma et al.
(2009)
(Fig. 3a)
“negative
feedback
loop with
buffer”

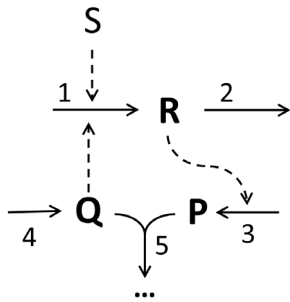
12



$$\begin{aligned} \frac{dP}{dt} &= k_1 S(1 - P) - k_2 P & P &= \frac{k_1 S}{k_1 S + k_2} & \text{Ma et al.} \\ \frac{dQ}{dt} &= k_5 P - k_6 Q & Q &= \frac{k_5}{k_6} \left(\frac{k_1 S}{k_1 S + k_2} \right) & (2009) \\ \frac{dR}{dt} &= k_3 P(1 - R) - k_4 Q R & R &= \frac{1}{1 + \frac{k_4 k_5}{k_3 k_6}} & (\text{Fig. 3b}) \\ \end{aligned}$$

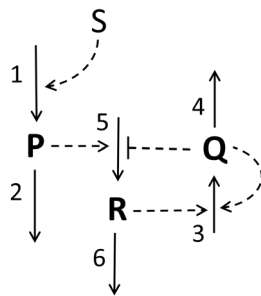
“incoherent feedforward loop”

13



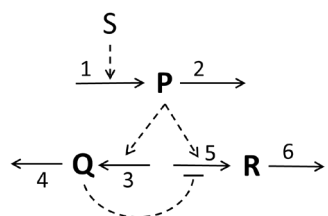
$$\begin{aligned} \frac{dP}{dt} &= k_3 R - k_5 P Q & P &= \frac{k_1 k_3 S}{k_2 k_5} & \text{Briat et al.} \\ \frac{dQ}{dt} &= k_4 - k_5 P Q & Q &= \frac{k_2 k_4}{k_3 k_1 S} & (2016) \\ \frac{dR}{dt} &= k_1 Q S - k_2 R & R &= \frac{k_4}{k_3} & \text{“N-type antithetic”} \\ \end{aligned}$$

14



$$\begin{aligned} \frac{dP}{dt} &= k_1 S - k_2 P & P &= \frac{k_1 S}{k_2} & \text{Shi et al.} \\ \frac{dQ}{dt} &= k_3 Q R - k_4 Q & 1 + Q &= \frac{k_1 k_3 k_5 S}{k_2 k_4 k_6} > 1 & (2017) \\ \frac{dR}{dt} &= \frac{k_5 P}{1 + Q} - k_6 R & R &= \frac{k_4}{k_3} & \text{“negative feedback loop with exponential buffer”} \\ \end{aligned}$$

15



$$\begin{aligned} \frac{dP}{dt} &= k_1 S - k_2 P & P &= \frac{k_1 S}{k_2} \ll K_3, K_5 & \text{Shi et al.} \\ \frac{dQ}{dt} &= k_3 \left(\frac{P}{K_3} \right)^{m_3} - k_4 Q & Q &= \frac{k_3}{k_4} \left(\frac{k_1 S}{k_2 K_3} \right)^{m_3} \gg L_5 & (2017) \\ \frac{dR}{dt} &= k_5 \left(\frac{P}{K_5} \right)^{m_5} \left(\frac{L_5}{Q} \right)^{n_5} - k_6 R & R &= & \text{“incoherent feedforward loop”} \\ & & & \frac{k_5}{k_6} \left(\frac{k_4 L_5}{k_3} \right)^{n_5} \frac{K_3^{m_3 n_5}}{K_5^{m_5}} \left(\frac{k_1 S}{k_2} \right)^{m_5 - m_3 n_5} & \\ & & \text{RPA if } m_3 n_5 = m_5 & & \end{aligned}$$

Supplementary Table S1. The *pure* signaling motifs.^a

Sign Pattern	Motif	Eight distinct cases	Name
0 0 ± 0 ± ±		(+ + -), (+ - +), (- + +), (- - -) (- - +), (- + -), (+ - -), (+ + +)	IFFL
			CFFL
± 0 ± 0 ± 0		(+ - +), (+ - -), (- + +), (- + -) (+ + +), (+ + -), (- - +), (- - -)	NFLB/upper
			PFLB/upper
0 0 0 ± ± ±		(+ + -), (+ - -), (- + +), (- - +) (+ + +), (+ - +), (- + -), (- - -)	NFLB/lower
			PFLB/lower
0 ± ± 0 0 ±		(+ + -), (+ - +), (- + +), (- - -) (+ - -), (- + -), (- - +), (+ + +)	NFL/ccw
			PFL/ccw
± 0 0 ± ± 0		(+ + -), (+ - +), (- + +), (- - -) (+ - -), (- + -), (- - +), (+ + +)	NFL/cw
			PFL/cw
Sign Pattern	Motifs	Explanatory Notes	
± ± 0 0 0 ± 0 0 ± ± 0 ± 0			Output node feeds back directly to input node. Regulatory node ineffective. Non-adaptive networks, according to Ma et al. (2009)
0 ± 0 ± ± 0 0 ± 0 0 ± ±			
± 0 ± 0 0 ± ± 0 0 ± ± 0 ±			Non-adaptive: regulatory node does not buffer the signal.
± 0 0 0 ± ± ± 0 0 ± ± ± 0			Non-adaptive: the output node receives direct influence from input node, but no corrective action from regulatory node.
0 ± ± ± 0 0 ± ± 0 ± 0 0			
± ± 0 0 0 ± ± ± 0 ± ± 0 0			Non-adaptive: the output node receives no influence, directly or indirectly, from input node. Therefore, no response to signal.
± 0 0 ± 0 ± ± 0 ± 0 ± 0 ±			

^a **Notes:** For a molecular interaction network with three links among three genes and/or proteins there are $6\text{-choose-}3 = 20$ different sign patterns with three 0's and three \pm 's, listed here. The sign patterns are translated into a motif diagram, where the connector ($j \rightarrow o i$) indicates that species j either activates or inhibits species i ($s_{ij} = \text{sign}(\omega_{ij}) = +$ for activation, $-$ for inhibition). The first five sign patterns are potentially adaptive motifs, with common names: IFFL, incoherent feedforward loop; CFFL, coherent feedforward loop; NFLB, negative feedback loop with buffer node; PFLB, positive feedback loop with buffer node; NFL, three-component negative feedback loop; PFL, three-component positive feedback loop; ccw, counterclockwise; cw, clockwise. The remaining 15 sign patterns are thought to be non-adaptive for the reasons given. In addition, CFFLs and PFLBs do not adapt on their own.

Supplementary Table S2. NFLB-1 topologies (1X3X3X) macro-mutate predominantly into high-scoring IFFL-1 + NFLB-1 topologies (1X3X31).

NFLB-1 Topologies	<u>IFFL-1 + NFLB-1 topologies</u>									
	113131	113231	113331	123131	123231	123331	133131	133231	133331	Others
113132	0	0	0.001	0	0.954	0.024	0.001	0.009	0.004	0.006
113133	0	0.004	0.001	0	0.957	0.008	0	0.022	0.001	0.007
113232	0	0	0	0	0.006	0.385	0	0.329	0.277	0.004
113233	0	0.001	0.002	0.001	0.651	0.331	0	0.007	0	0.006
113332	NA	NA	NA	NA	NA	NA	NA	NA	NA	NA
113333	0	0	0	0.010	0.110	0.108	0.000	0.018	0.754	0
123132	0	0	0	0	0.055	0.010	0.001	0.015	0.917	0.001
123133	0.001	0.007	0	0.459	0.214	0.011	0.043	0.161	0.097	0.007
<i>123232</i>	0	0	0	0.005	0.189	0.008	0.001	0.788	0.006	0.005
123233	0	0	0	0.001	0.321	0.019	0.001	0.652	0.007	0
123332	0	0	0.000	0.001	0.210	0.352	0.001	0.004	0.431	0
123333	0	0	0	0.001	0.976	0.015	0	0.007	0.002	0
133132	0	0	0.002	0.005	0.020	0.359	0	0.106	0.505	0.002
133133	0.001	0	0	0.471	0.003	0	0.476	0.030	0.014	0.005
133232	0	0	0	0	0.003	0.004	0.002	0.543	0.447	0
133233	NA	NA	NA	NA	NA	NA	NA	NA	NA	NA
133332	0	0.000	0.000	0.001	0.320	0.280	0.000	0.393	0.004	0.001
133333	0	0	0	0.000	0.278	0.346	0	0.206	0.169	0

The *pure* NFLB-1 (123232) is marked in *italics*. Bold percentages indicate cases where an IFFL-1 + NFLB-1 topology occupies more than 15% of the high-scoring sample in a macro-mutation run. Percentages bordered in red indicate cases where a topology occupies more than 50% of the high-scoring sample. NA means no high-scoring topologies were found.

Supplementary Table S3. NFLB-3 topologies (XXX331) macro-mutate predominantly into high-scoring IFFL-1 + NFLB-1 topologies (1X3X31).

NFLB-3 Topologies	IFFL-1 + NFLB-1 Topologies									
	113131	113231	113331	123131	123231	123331	133131	133231	133331	Others
111331	0.001	0.004	0.564	0	0.372	0.047	0	0.007	0	0.005
112331	0	0	0.009	0			0.001	0.007	0.005	0.006
121331	0	0.001	0	0.005			0	0.006	0	0.007
122331	0	0	0.002	0	0.038		0	0	0.006	0.006
131331	0	0	0	0.001	0.031		0	0	0.006	0.005
132331	0	0.001	0.002	0.001	0.031		0.001	0.001	0.247	0.025
211331	0	0	0	0	0	0.003	0	0.409	0.588	0
212331	0	0.003	0	0.001	0.001	0.002	0.001	0	0	0.992^a
221331	0	0.003	0	0.001	0.109		0	0.001	0.005	0.005
222331	0	0	0	0.002	0.004		0	0.001	0.005	0.001
231331	0	0.002	0	0		0.029	0	0.006	0.002	0.002
232331	0	0.003	0.001	0	0.012	0.008	0	0.021		0.003
312331	0	0	0	0	0.006	0.006	0.002			0.002
322331	0	0.001	0.003	0.007	0.028		0	0.042	0.005	0.002
332331	0.001	0.004	0	0			0	0.429	0.003	0.013

The *pure* NFLB-3 (222331) is marked in *italics*. Bold percentages indicate cases where an IFFL-1 + NFLB-1 topology occupies more than 15% of the high-scoring sample in a macro-mutation run. Percentages bordered in red indicate cases where a topology occupies more than 50% of the high-scoring sample. NA means no high-scoring topologies were found.

^aIn this case, the predominant endpoints are IFFL-1 only (213231, 223231, 323231) and IFFL-1 + NFLB-3 (323331 and 333331).

Supplementary Table S4. NFLB-2 topologies (3X1X3X) macro-mutate predominantly to high-scoring IFFL-1 + NFLB-1 topologies (1X3X31). *Italic*: the *pure* NFLB-2 (321232); **bold**: more than 15% of cases in an IFFL-1 + NFLB-1 topology. NA means no high-scoring topologies were found.

NFLB-2 Topologies	IFFL-1 + NFLB-1 Topologies									
	113131	113231	113331	123131	123231	123331	133131	133231	133331	Others
311131	0	0.005	0.317			0.045	0	0.003	0	0.011
311132	0.001	0	0		0.015	0.002	0.117	0.005	0.004	0.016
311231	0.001	0	0	0.128	0.015	0.002	0	0.002	0	0.853^a
311232	0	0	0	0	0.017	0.326	0	0.010	0.646	0.002
311331	0	0.001	0	0	0.006	0	0.003	0.946	0.011	0.033
311332	NA	NA	NA	NA	NA	NA	NA	NA	NA	NA
321131	0.001	0.006	0.004	0	0.399	0.578	0	0.001	0.004	0.008
321132	NA	NA	NA	NA	NA	NA	NA	NA	NA	NA
321231	NA	NA	NA	NA	NA	NA	NA	NA	NA	NA
321232	0	0	0	0	0	0	0	0	0	1.000^b
321331	0	0.001	0.002	0.013	0.293	0.682	0	0.001	0.001	0.007
321332	0.005	0.003	0	0.016	0.635	0.328	0	0.003	0.003	0.006
331131	0.527	0.003	0.005	0.448	0.005	0.002	0.003	0.002	0	0.005
331132	0	0.004	0.501	0.001	0.116	0.331	0	0	0.037	0.009
331231	0.002	0.220	0.002	0	0.005	0.008	0.001	0.230	0.520	0.011
331232	NA	NA	NA	NA	NA	NA	NA	NA	NA	NA
331331	NA	NA	NA	NA	NA	NA	NA	NA	NA	NA
331332	0	0.001	0	0	0.973	0.004	0	0.018	0	0.005

^aThe dominant topologies in this case are *uncoupled* NFLB-1: 133232, 123232 and 123132.

^bThe dominant topologies in this case are IFFL-4 + NFLB-2: 331333, 321233 and 321133.

Supplementary Table S5. NFLB-4 topologies (XXX133) macro-mutate predominantly to high-scoring IFFL-1 + NFLB-1 topologies (1X3X31). *Italic*: the *pure* NFLB-2 (321232); **bold**: more than 15% of cases in an IFFL-1 + NFLB-1 topology. NA means no high-scoring topologies were found.

NFLB-4 Topologies	IFFL-1 + NFLB-1 Topologies									
	113131	113231	113331	123131	123231	123331	133131	133231	133331	Others
112133	0	0	0	0	0	0.003	0	0.008	0.989	0
122133	0	0	0	0	0.015	0.001	0	0.974	0.009	0.001
132133	0	0	0.001	0.004	0.878	0.006	0	0.007	0.004	0.101
212133	0	0	0	0.003	0.096	0.004	0	0.001	0	0.896^a
213133	0.005	0	0	0.644	0.329	0.005	0.011	0.003	0.002	0.003
223133	NA	NA	NA	NA	NA	NA	NA	NA	NA	NA
222133	0	0	0	0	0	0	0	0	0	1.000^b
232133	0	0.003	0.051	0	0.436	0.503	0	0.001	0.006	0
233133	0	0	0	0.063	0	0.003	0.905	0.018	0.003	0.010
312133	0	0	0	0	0.006	0.014	0	0.250	0.729	0.001
313133	0	0	0	0	0.007	0.003	0.254	0.707	0.026	0.002
322133	0.001	0.004	0.001	0	0.476	0.001	0.001	0.198	0.313	0.005
323133	0	0	0	0	0	0.013	0	0.008	0.975	0.004
332133	0	0	0	0.001	0.013	0.119	0	0.533	0.331	0.003
333133	0	0	0.001	0.002	0.606	0.377	0	0.005	0.007	0.002

^aThe dominant topologies in this case are *uncoupled* NFLB-1: 123332 and 123232.

^bThe dominant topologies in this case are IFFL-4 + NFLB-2: 331133 and 321133.

Supplementary Table S6. The percentage change in average score $\langle Z \rangle$ going from an *uncoupled* NFLB-1 topology to a coupled NFLB-1 + IFFL-1 topology. Note: the last digit changes to 1 in each case. The average change overall is +52%.

NFLB-1 only Code	$\langle Z \rangle$	NFLB-1 + IFFL-1 Code	$\langle Z \rangle$	Percentage Change
113132	9.35	113131	16.87	80
113133	8.63	113131	16.87	95
113232	10.32	113231	16.26	58
113233	8.73	113231	16.26	86
113332	10.69	113331	16.10	51
113333	8.97	113331	16.10	79
123132	12.06	123131	16.92	40
123133	10.46	123131	16.92	62
123232	9.80	123231	17.15	75
123233	10.55	123231	17.15	63
123332	12.29	123331	16.76	36
123333	10.71	123331	16.76	56
133132	15.40	133131	17.68	15
133133	13.20	133131	17.68	34
133232	15.00	133231	17.03	14
133233	12.48	133231	17.03	36
133332	14.29	133331	16.77	17
133333	11.99	133331	16.77	40

Supplementary Table S7. The percentage change in average score $\langle Z \rangle$ going from an *uncoupled* NFLB-2 topology to a coupled NFLB-2 + IFFL-4 topology. Note: the last digit changes to 3 in each case. The average change overall is +240%.

NFLB-2 only		NFLB-2 + IFFL-4		Percentage Change
Code	$\langle Z \rangle$	Code	$\langle Z \rangle$	
311131	1.64	311133	13.64	732
311132	6.23	311133	13.64	119
311231	4.55	311233	10.4	129
311232	4.74	311233	10.4	119
311331	2.79	311333	11.81	323
311332	4.3	311333	11.81	175
321131	1.33	321133	12.94	873
321132	7.39	321133	12.94	75
321231	5.09	321233	12.9	153
321232	7.1	321233	12.9	82
321331	4.55	321333	12.53	175
321332	4.42	321333	12.53	183
331131	4.73	331133	12.55	165
331132	7.58	331133	12.55	66
331231	4.76	331233	14.36	202
331232	4.78	331233	14.36	200
331331	2.8	331333	14.34	412
331332	8.2	331333	14.34	75

Supplementary Table S8. The percentage change in average score $\langle Z \rangle$ going from an *uncoupled* NFLB-3 topology to a coupled NFLB-3 + IFFL-1 topology. Note: the third digit changes to 3 in each case. The average change overall is +290%.

NFLB-3 only Code	$\langle Z \rangle$	NFLB-3 + IFFL-1 Code	$\langle Z \rangle$	Percentage Change
111331	2.13	113331	16.1	656
112331	5.05	113331	16.1	219
121331	4.19	123331	16.76	300
122331	5.67	123331	16.76	196
131331	3.91	133331	16.77	329
132331	5.67	133331	16.77	196
211331	2.4	213331	10.93	355
212331	3.39	213331	10.93	222
221331	2.49	223331	9.34	275
222331	3.13	223331	9.34	198
231331	2.77	233331	14.99	441
232331	2.96	233331	14.99	406
311331	2.8	313331	10.33	269
312331	3.35	313331	10.33	208
321331	4.55	323331	14.91	228
322331	3.36	323331	14.91	344
331331	2.8	333331	9.19	228
332331	3.11	333331	9.19	195

Supplementary Table S9. The percentage change in average score $\langle Z \rangle$ going from an *uncoupled* NFLB-4 topology to a coupled NFLB-4 + IFFL-4 topology. Note: the third digit changes to 1 in each case. The average change overall is +330%.

NFLB-4 only Code	$\langle Z \rangle$	NFLB-4 + IFFL-4 Code	$\langle Z \rangle$	Percentage Change
112133	2.74	111133	12.48	355
113133	8.63	111133	12.48	45
122133	2.68	121133	11.96	346
123133	10.46	121133	11.96	14
132133	2.59	131133	12.57	385
133133	13.2	131133	12.57	-5
212133	2.64	211133	11.41	332
213133	2.24	211133	11.41	409
222133	2.64	221133	13.67	418
223133	2.27	221133	13.67	502
232133	2.12	231133	11.27	432
233133	2.43	231133	11.27	364
312133	2.9	311133	13.64	370
313133	2.6	311133	13.64	425
322133	3.25	321133	12.94	298
323133	2.63	321133	12.94	392
332133	3.22	331133	12.55	290
333133	1.81	331133	12.55	593

Supplementary Table S10. The percentage changes in average score $\langle Z \rangle$ going from an *uncoupled* IFFL-1 topology to a coupled IFFL-1 + NFLB-1 topology. Note: the first digit changes to 1 in each case. The average change overall is +23%.

IFFL-1 only		NFLB-1 + IFFL-1		Percentage Change
Code	$\langle Z \rangle$	Code	$\langle Z \rangle$	
213131	11.43	113131	16.87	48
313131	13.14	113131	16.87	28
213231	13.19	113231	16.26	23
313231	14.73	113231	16.26	10
223131	15.18	123131	16.92	11
323131	10.80	123131	16.92	57
223231	15.25	123231	17.15	12
323231	15.62	123231	17.15	10
233131	13.88	133131	17.68	27
333131	15.49	133131	17.68	14
233231	14.38	133231	17.03	18
333231	14.40	133231	17.03	18

Supplementary Table S11. The percentage changes in average score $\langle Z \rangle$ going from an *uncoupled* IFFL-1 topology to a coupled IFFL-1 + NFLB-3 topology. Note: the fourth digit changes to 3 in each case. The average change overall is -15% .

IFFL-1 only		NFLB-3 + IFFL-1		Percentage Change
Code	$\langle Z \rangle$	Code	$\langle Z \rangle$	
213131	11.43	213331	10.93	-4
213231	13.19	213331	10.93	-17
223131	15.18	223331	9.34	-38
223231	15.25	223331	9.34	-39
233131	13.88	233331	14.99	8
233231	14.38	233331	14.99	4
313131	13.14	313331	10.33	-21
313231	14.73	313331	10.33	-30
323131	10.8	323331	14.91	38
323231	15.62	323331	14.91	-5
333131	15.49	333331	9.19	-41
333231	14.4	333331	9.19	-36

Supplementary Table S12. The percentage changes in average score $\langle Z \rangle$ going from an *uncoupled* IFFL-1 topology to a coupled IFFL-1 + NFLB-1 + NFLB-3 topology. Note: first digit = 1, fourth digit = 3 in each case. The average change overall is +20%.

IFFL-1 only		NFLB-1 + NFLB-3		Percentage Change
Code	$\langle Z \rangle$	+ IFFL-1 Code	$\langle Z \rangle$	
213131	11.43	113331	16.1	41
213231	13.19	113331	16.1	22
313131	13.14	113331	16.1	23
313231	14.73	113331	16.1	9
223131	15.18	123331	16.76	10
223231	15.25	123331	16.76	10
323131	10.8	123331	16.76	55
323231	15.62	123331	16.76	7
233131	13.88	133331	16.77	21
233231	14.38	133331	16.77	17
333131	15.49	133331	16.77	8
333231	14.4	133331	16.77	16

Supplementary Table S13. The percentage changes in average score $\langle Z \rangle$ adding an NFLB-3 topology to a coupled IFFL-1 + NFLB-1 topology. Note: fourth digit = 3 in each case. The average change overall is -2.6% .

NFLB-1 + IFFL-1		NFLB-1 + NFLB-3 + IFFL-1		Percentage Change
Code	$\langle Z \rangle$	Code	$\langle Z \rangle$	
113131	16.87	113331	16.1	-4.6
113231	16.26	113331	16.1	-1.0
123131	16.92	123331	16.76	-0.9
123231	17.15	123331	16.76	-2.3
133131	17.68	133331	16.77	-5.1
133231	17.03	133331	16.77	-1.5

Supplementary Table S14. The percentage changes in average score $\langle Z \rangle$ adding an NFLB-1 topology to a coupled IFFL-1 + NFLB-3 topology. Note: first digit = 1 in each case. The average change overall is +48%.

NFLB-3 + IFFL-1		NFLB-1 + NFLB-3 + IFFL-1		Percentage Change
Code	$\langle Z \rangle$	Code	$\langle Z \rangle$	
213331	10.93	113331	16.1	47
313331	10.33	113331	16.1	56
223331	9.34	123331	16.76	79
323331	14.91	123331	16.76	12
233331	14.99	133331	16.77	12
333331	9.19	133331	16.77	82

Supplementary Table S15. The percentage changes in average score $\langle Z \rangle$ going from an *uncoupled* IFFL-4 topology to a coupled IFFL-4 + NFLB-2 topology. Note: first digit = 3 in each case. The average change overall is +3.8%.

IFFL-4 only		NFLB-2 + IFFL-4		Percentage Change
Code	$\langle Z \rangle$	Code	$\langle Z \rangle$	
111233	11.45	311233	12.73	11.2
211233	11.89	311233	12.73	7.1
111333	14.04	311333	11.81	-15.9
211333	13.25	311333	11.81	-10.9
121233	12.02	321233	12.9	7.3
221233	11.96	321233	12.9	7.9
121333	13.47	321333	12.53	-7.0
221333	12.15	321333	12.53	3.1
131233	13.64	331233	14.36	5.3
231233	12.19	331233	14.36	17.8
131333	13.55	331333	14.34	5.8
231333	12.61	331333	14.34	13.7

Supplementary Table S16. The percentage changes in average score $\langle Z \rangle$ going from an *uncoupled* IFFL-4 topology to a coupled IFFL-4 + NFLB-4 topology. Note: fourth digit = 1 in each case. The average change overall is -3.2%.

IFFL-4 only		NFLB-4 + IFFL-4		Percentage Change
Code	$\langle Z \rangle$	Code	$\langle Z \rangle$	
111233	11.45	111133	12.48	9.0
111333	14.04	111133	12.48	-11.1
211233	11.89	211133	11.41	-4.0
211333	13.25	211133	11.41	-13.9
121233	12.02	121133	11.96	-0.5
121333	13.47	121133	11.96	-11.2
221233	11.96	221133	13.67	14.3
221333	12.15	221133	13.67	12.5
131233	13.64	131133	12.57	-7.8
131333	13.55	131133	12.57	-7.2
231233	12.19	231133	11.27	-7.5
231333	12.61	231133	11.27	-10.6

Supplementary Table S17. The percentage changes in average score $\langle Z \rangle$ going from an *uncoupled* IFFL-4 topology to a coupled IFFL-4 + NFLB-2 + NFLB-4 topology. Note: first digit = 3, fourth digit = 1 in each case. The average change overall is +3.3%.

IFFL-4 only		NFLB-2 + NFLB-4 + IFFL-4		Percentage Change
Code	$\langle Z \rangle$	Code	$\langle Z \rangle$	
111233	11.45	311133	13.64	19.1
211233	11.89	311133	13.64	14.7
111333	14.04	311133	13.64	-2.8
211333	13.25	311133	13.64	2.9
121233	12.02	321133	12.94	7.7
221233	11.96	321133	12.94	8.2
121333	13.47	321133	12.94	-3.9
221333	12.15	321133	12.94	6.5
131233	13.64	331133	12.55	-8.0
231233	12.19	331133	12.55	3.0
131333	13.55	331133	12.55	-7.4
231333	12.61	331133	12.55	-0.5

Supplementary Table S18. The percentage changes in average score $\langle Z \rangle$ adding an NFLB-4 topology to a coupled IFFL-4 + NFLB-2 topology. Note: fourth digit = 1 in each case. The average change overall is +0.2%.

NFLB-2 + IFFL-4		NFLB-2 + NFLB-4 + IFFL-4		Percentage Change
Code	$\langle Z \rangle$	Code	$\langle Z \rangle$	
311233	12.73	311133	13.64	7.1
311333	11.81	311133	13.64	15.5
321233	12.9	321133	12.94	0.3
321333	12.53	321133	12.94	3.3
331233	14.36	331133	12.55	-12.6
331333	14.34	331133	12.55	-12.5

Supplementary Table S19. The percentage changes in average score $\langle Z \rangle$ adding an NFLB-2 topology to a coupled IFFL-4 + NFLB-4 topology. Note: first digit = 3 in each case. The average change overall is +7.1%.

NFLB-4 + IFFL-4		NFLB-2 + NFLB-4 + IFFL-4		Percentage Change
Code	$\langle Z \rangle$	Code	$\langle Z \rangle$	
111133	12.48	311133	13.64	9.3
211133	11.41	311133	13.64	19.5
121133	11.96	321133	12.94	8.2
221133	13.67	321133	12.94	-5.3
131133	12.57	331133	12.55	-0.2
231133	11.27	331133	12.55	11.4

Supplementary Table S20. Mean values of the six interaction coefficients from all high-scoring samples of IFFL-1 topologies.

IFFL-1 Code	Interaction Coefficients					
	ω_{12}	ω_{13}	ω_{21}	ω_{23}	ω_{31}	ω_{32}
113131	-0.98	-0.14	0.89	-0.20	0.97	-0.96
113231	-1.00	-0.13	0.93	0.00	0.95	-0.98
113331	-0.97	-0.13	0.85	0.26	0.97	-0.88
123131	-0.99	0.00	0.88	-0.17	0.97	-0.95
123231	-0.99	0.00	0.89	0.00	0.97	-0.96
123331	-1.00	0.00	0.95	0.16	0.97	-0.99
133131	-0.92	0.52	0.82	-0.16	0.97	-0.63
133231	-0.85	0.62	0.54	0.00	0.97	-0.90
133331	-0.84	0.50	0.85	0.30	0.97	-0.64
213131	0.00	-0.13	0.93	-0.29	0.95	-0.97
213231	0.00	-0.16	0.92	0.00	0.96	-0.98
213331	0.00	-0.19	0.56	0.17	0.66	-0.96
223131	0.00	0.00	0.90	-0.34	0.96	-0.98
223231	0.00	0.00	0.89	0.00	0.96	-0.98
223331	0.00	0.00	0.52	0.79	0.97	-0.95
233131	0.00	0.27	0.90	-0.28	0.95	-0.97
233231	0.00	0.20	0.92	0.00	0.97	-0.98
233331	0.00	0.29	0.91	0.34	0.97	-0.98
313131	0.20	-0.15	0.91	-0.33	0.96	-0.97
313231	0.27	-0.23	0.92	0.00	0.97	-0.98
313331	0.15	-0.21	0.58	0.24	0.68	-0.96
323131	0.12	0.00	0.48	-0.20	0.64	-0.95
323231	0.33	0.00	0.92	0.00	0.97	-0.98
323331	0.27	0.00	0.91	0.19	0.97	-0.98
333131	0.18	0.38	0.90	-0.25	0.96	-0.98
333231	0.27	0.36	0.92	0.00	0.97	-0.98
333331	0.23	0.30	0.62	0.37	0.68	-0.96

Red, the ω_{ij} 's for the three links of the underlying IFFL-1; **blue**, the ω_{12} 's in the NFLB-1 cases; **purple**, the ω_{23} 's in the NFLB-3 cases.

Supplementary Table 21. Mean values of the six interaction coefficients from all high-scoring samples of IFFL-4 topologies.

IFFL-4 Code	Interaction Coefficients					
	ω_{12}	ω_{13}	ω_{21}	ω_{23}	ω_{31}	ω_{32}
111133	-0.30	-0.22	-0.87	-0.21	0.95	0.96
111233	-0.39	-0.16	-0.86	0.00	0.95	0.96
111333	-0.43	-0.14	-0.86	0.25	0.94	0.96
121133	-0.29	0.00	-0.88	-0.26	0.95	0.97
121233	-0.27	0.00	-0.88	0.00	0.96	0.97
121333	-0.48	0.00	-0.83	0.22	0.93	0.96
131133	-0.16	0.30	-0.90	-0.24	0.95	0.97
131233	-0.31	0.47	-0.89	0.00	0.95	0.97
131333	-0.50	0.38	-0.89	0.14	0.94	0.97
211133	0.00	-0.21	-0.88	-0.25	0.96	0.97
211233	0.00	-0.16	-0.87	0.00	0.96	0.96
211333	0.00	-0.21	-0.88	0.25	0.95	0.96
221133	0.00	0.00	-0.90	-0.17	0.96	0.97
221233	0.00	0.00	-0.88	0.00	0.95	0.97
221333	0.00	0.00	-0.85	0.21	0.94	0.96
231133	0.00	0.30	-0.87	-0.15	0.95	0.97
231233	0.00	0.46	-0.82	0.00	0.94	0.96
231333	0.00	0.37	-0.87	0.20	0.95	0.96
311133	0.88	-0.13	-0.81	-0.18	0.95	0.66
311233	0.23	-0.15	-0.83	0.00	0.95	0.95
311333	0.15	-0.27	-0.84	0.14	0.95	0.96
321133	0.83	0.00	-0.77	-0.49	0.94	0.70
321233	0.90	0.00	-0.82	0.00	0.95	0.67
321333	0.85	0.00	-0.84	0.18	0.94	0.61
331133	0.61	0.34	-0.82	-0.31	0.95	0.71
331233	0.83	0.29	-0.83	0.00	0.94	0.57
331333	0.77	0.45	-0.82	0.15	0.94	0.59

Green, the ω_{ij} 's for the three links of the underlying IFFL-4; blue, the ω_{12} 's in the NFLB-2 cases; purple, the ω_{23} 's in the NFLB-4 cases.